# ChemComm

Accepted Manuscript


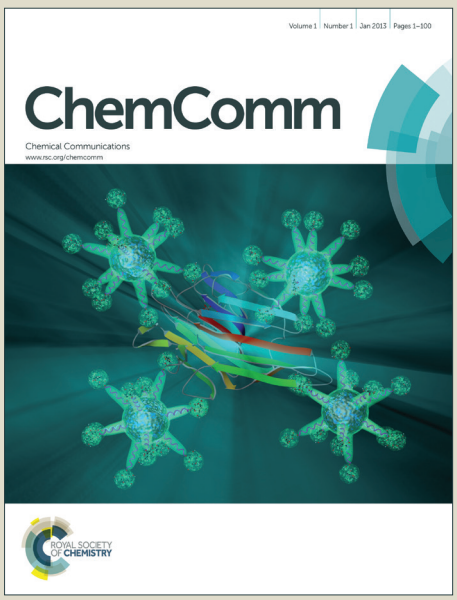





ROYAL SOCIETY OF CHEMISTRY

www.rsc.org/chemcomm

Journal Name

RSCPublishing

COMMUNICATION

# Lithium anode protection guided highly-stable lithium-sulfur battery

Cite this: DOI: 10.1039/x0xx00000x

Guoqiang Ma [a], Zhaoyin Wen* [a], Meifen Wu [a], Chen Shen [a], Qingsong Wang [a], Jun Jin [a], Xiangwei Wu [a]

Received 00th January 2012,
Accepted 00th January 2012

DOI: 10.1039/x0xx00000x

www.rsc.org/

**$Li_3N$ protection layer is fabricated on the surface of Li anode by an in-situ method to suppress the shuttle effect on the basis of anode protection. The discharge capacity retains at 773 mAh.g$^{-1}$ after 500 cycles with the average coulombic efficiency of 92.3% in the electrolyte without $LiNO_3$, while the sulfur loading of the simple sulfur cathode was 2.5-3 mg cm$^{-2}$.**

With rapid development in the advanced portable devices, zero-emission electric vehicles (EV) and smart grids, rechargeable batteries with high energy density and long cycle life have been given great demand[1, 2]. Sulfur cathode has a high theoretical capacity (1675 mAh.g$^{-1}$), which is ~5 times that of existing materials based on layered lithium transition metal oxides and lithium metal phosphates. In combination with the natural abundance, low cost and environmental friendliness of sulfur, the Li-S battery becomes a promising candidate for the next generation power source[3-5].

However，the commercialization of Li-S battery is inhibited by the insulating nature of sulfur, the volume expansion, and the high solubility of lithium polysulfides (PS) in the ether-based electrolyte[6-8]. The shuttle effect originates from the diffusion of high order polysulfides to the anode side, where they react with metal lithium and form the insoluble $Li_2S/Li_2S_2$, which irreversibly deposit on the surface of the lithium anode. Such corrosion reaction causes the loss of active sulfur materials, leading to low coulombic efficiency, rapid capacity fading and high polarization[9, 10]. Furthermore, complete conversion of sulfur to $Li_2S$ is difficult owing to the insulating feature of $Li_2S/Li_2S_2$. Besides, there is some irreversible capacity for Li-S battery because of the side reaction during the charge/discharge process[11].

Many approaches have been made to solve the problems and improve the electrochemical performance of Li-S battery, including the micro structural design of the cathode[12, 13], the modification of the electrolyte[10]and so on. Encapsulating sulfur into conductive matrix[21-23] and the surface coating of sulfur or sulfur composite with conductive materials[13] are most frequently employed to address these obstacles. The conductive material such as various of carbon and conductive polymer can improve the electrical conductivity of the cathode and suppress the loss of soluble polysulfides intermediates, and thereby improve the active material utilization and cycle stability[6]. In addition, the issue of low coulombic efficiency has been resolved by the addition of lithium nitrate in the electrolyte[16]. However, up to now, few researches on lithium anode for Li-S battery are reported, the modification of the lithium electrode should be a new strategy to improve the performance of Li-S battery[6, 7].

Li anode for Li-S battery suffers from several problems. Firstly, lithium is so reactive that the electrolyte can be reduced on the surface of the Li anode to form a solid electrolyte interphase (SEI) layer easily, causing a great irreversible capacity loss and low deposition efficiency of Li upon charging[17-19]. Secondly, the Li dendrites originated from the no uniform deposition of Li deteriorate Li-metal based battery life and even cause safety problem[20, 21]. While the lithium polysulfides in the electrolyte may react with Li dendrites, thus the problem is not as serious as the other Li anode based battery[22]. Thirdly, as shown in Fig.1a, the shuttle effect in Li-S battery, the penetration of soluble lithium polysulfides through the separator will react with Li anode to form the $Li_2S/Li_2S_2$ layer on the surface of lithium anode[8, 23]. Then the insulating $Li_2S/Li_2S_2$ on the surface of Li anode is difficult to be transformed to lithium polysulfides and utilized at the following cycles, leading to the loss of the active material[24]. Furthermore, the insulating layer will retard the rapid diffusion of Li, resulting in poor rate capability and cycle performance[21]. Li-B alloy, Lithium ion conductive solid polymer electrolyte and sulfur powder coating have been employed to protect Li anode during charge/discharge process[25-27].

Polycrystalline $Li_3N$ has an exceptionally high Li-ion conductivity (approximately $10^{-3}$ S.cm$^{-1}$) with potential application as a solid electrolyte in lithium ion batteries[28-30]. As the closest layer to Li
metal, $Li_3N$ can prevent the side reaction between the lithium and the carbonate-based electrolyte, promoting an stable SEI[29]. Furthermore, fast $Li^+$ diffusion from electrolyte to Li surface is built owing to fewer reduction species in the electrolyte with $Li_3N$ modification on the Li anode surface. Thus it is proposed to employ $Li_3N$ as the protecting layer to address the obstacles of Li anode for Li-S battery in this work.

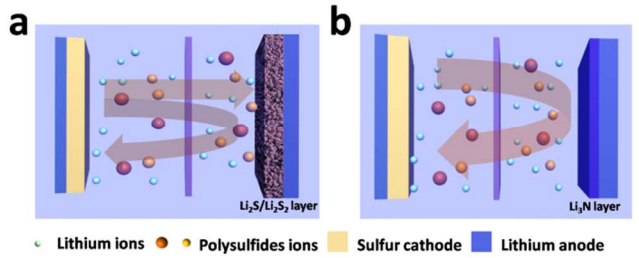


Figure. 1 Schematic of the design of lithium metal electrode in lithium-sulfur battery configurations. (a) Battery without $Li_3N$ layer. (b) Battery with $Li_3N$ layer.

Herein, As seen in Fig.1b, $Li_3N$ protecting layer is in-situ fabricated on the surface of Lithium anode by the direct reaction between the Li and $N_2$ gas at room temperature. Firstly, $Li_3N$ layer has a high ionic conductivity, which doesn't hinder the migration of $Li^+$. Secondly, $Li_3N$ layer can prevent the side reaction between lithium anode and the electrolyte, forming a stable SEI layer. Thirdly, the contact between the lithium polysulfides and lithium anode is thus prevented, and the undesired corrosive reaction is suppressed. As a result, the migration of lithium polysulfides back to the cathode and reutilization of them at the following cycles are possible, inhibition of capacity fading is thus realized. Furthermore, the Li dendrites originating from an no uniform deposition of Li can be suppressed by the $Li_3N$ layer, improving the safety of the battery.

As shown in Fig.S1, the phase of $Li_3N$ film formed on Li surface is characterized by XRD analysis. The pure $Li_3N$ is fabricated on the surface of Li foil with the simple method, and it is stable in the ether-based electrolyte after 10 days[30, 31]. The morphologies of the as-received Li and $Li_3N$ modified Li electrodes are given in Fig. S2. As seen, both electrode surfaces are homogeneous. It is noticeable that the modified surface is strongly charged by the electron beam since the $Li_3N$ film is electronically insulated.

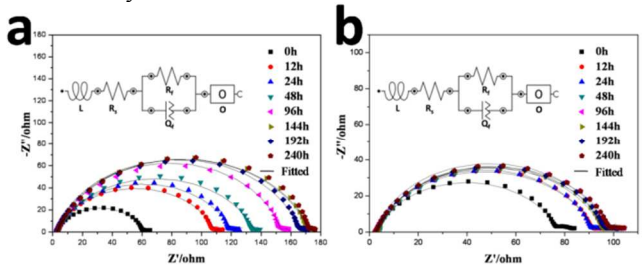


**Figure. 2** AC impedance spectra of the Li/electrolyte/Li batteries with (a) as received Li and (b) surface protected Li electrodes as a function of storage time at 25◦C.

The lithium sheet with $Li_3N$ layer is beneficial to form a stable and less resistive SEI in the carbonate-based electrolyte[29]. To investigate the interfacial stability of the $Li_3N$ protected lithium anode in the ether-based electrolyte, AC impedance measurement for Li/electrolyte/Li batteries is performed[17]. As seen in Fig.2, the spectra are composed of a partially overlapping semicircles, corresponding to the SEI film. The equivalent circuit and related analogs fitted to the experimental data are also given in Fig.2.

In this circuit, $R_s$ is the electrolyte resistance, which corresponds to the high frequency intercept at the real axis. $R_f$ is the resistance of the SEI film[17]. In the battery assembled with the primitive Li electrode, the initial resistance of the battery is less than those of the Li electrode with $Li_3N$ layer, indicating the existence of protective layer on the surface of lithium anode. However, the $R_f$ value increases from 59Ω to 168 Ω after 144h, owing to the gradual growth of SEI between the lithium electrode and the electrolyte. In the battery assembled with the $Li_3N$ protected Li electrode, $R_f$ initially increases to the maximum value after 48h and stabilizes at around 92Ω. $R_f$ stabilizes at a less value after a shorter storage time compared to that of the as received Li anode, indicating the suppressed undesired side reactions between $Li_3N$ protected lithium electrode and the ether-based electrolyte. As a result, the interfacial stability of the lithium electrode is improved by the formation of $Li_3N$ protection layer.

The fitted results of the impedance spectra in Fig.2a and Fig.2b are given in Table.S1 and Table. S2, respectively. Among them, $B=l/D^{1/2}$, where l is the length of stagnant layer and D is diffusion coefficient. According to the previous studies, the diffusion coefficient of $Li^+$ in the electrolyte is about $3.4\times10^{-6}$ $cm^2S^{-1}$, thus the value of l can be calculated[32]. As shown, The goodness fit for the whole electrode system is represented by the Chi-square ($\chi^2$) parameter. Comparing $R_f$ and $Q_f$ in the two table, it indicates that the SEI formed on $Li_3N$ protected Li anode surface is smoother and less resistive. As $Li_3N$ protective layer is formed previously and used as the close layer to Li sheet, it can effectively prevent the side reactions between Li and electrolyte. Moreover, the high Li conductivity of $Li_3N$ can provide much smaller $Li^+$ migration resistance $R_f$. It is noticeable that the larger value $Y_0$ of "Cothyperbol" element O and shorter lengths of stagnant layers suggest fast $Li^+$ diffusion from electrolyte to Li surface, owing to fewer reduction species in the electrolyte with $Li_3N$ modification.

The cyclic voltammogram (CV) profiles are measured to identify the redox reactions for the battery with different anodes (Fig. S3a and b). The electrochemical activation of $Li_3N$ protected anode is not as obvious as that of the primitive Li anode. Which can be ascribed to the faster $Li^+$ diffusion from electrolyte to Li surface with the modification of $Li_3N$, owing to fewer reduction species in the electrolyte with $Li_3N$ modification, which is consistent with the results of AC impedance.

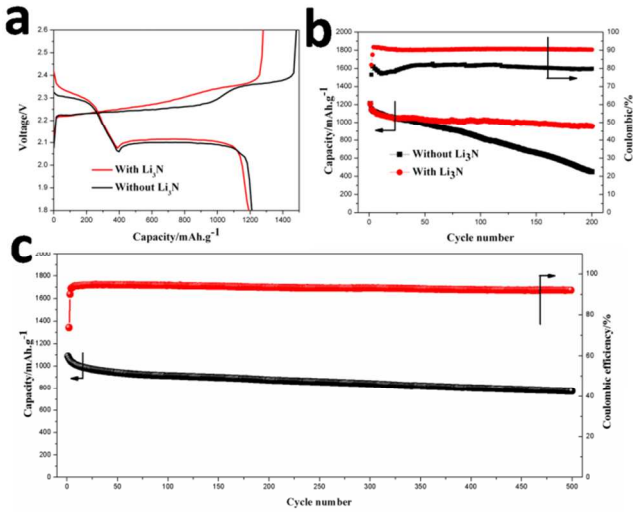


**Figure. 3** The initial charge/discharge profiles of Li-S batteries with different lithium anodes at 0.2C(a), the cycle performance and coulombic efficiencies of Li-S batteries at 0.2C with different lithium anodes (b), the prolonged cycle performance and coulombic efficiencies of Li-S batteries at 0.5C with $Li_3N$ layer protected Li anode (c).

In a coin type battery for electrochemical test, lithium anode is normally far from sufficient with respect to the active material in the sulfur cathode, so the initial discharge capacity is determined by the state of sulfur cathode. As seen in Fig.3a, the Li-S battery with primitive Li electrode shows a comparable initial discharge capacity with that of Li-S battery with $Li_3N$ protected lithium anode. However, the two discharge potential plateaus of battery with $Li_3N$ protected anode are higher than those of the battery with primitive Li anode, meanwhile the charge potential plateau is lower for the battery with $Li_3N$ protected anode, further proving its lower polarization of the $Li_3N$ protected anode in the ether-based electrolyte.

The cycle performance and coulombic efficiencies of Li-S batteries at 0.2C with different lithium electrodes are shown in Fig.3b. As mentioned above, once lithium anode is protected by $Li_3N$ layer, the contact between lithium anode and lithium polysulfides can be restricted, so the corrosive reaction between them during the discharge process is suppressed effectively. Furthermore, because of the high $Li^+$ conductivity of $Li_3N$, more insulating $Li_2S/Li_2S_2$ aggregated on the surface of the conductive $Li_3N$ layer will transform to the soluble $Li_2S_x$ during the charge process. Consequently, the so called "shuttle effect" is largely restricted, thus the low coulombic efficiencies, redistribution of active material and rapid capacity fading are suppressed significantly. As shown, the discharge capacity of Li-S battery with $Li_3N$ protected Li anode remains as high as 956.6 $mAh.g^{-1}$ at 0.2C with a capacity retention of 79.7% after 200 cycles, while Li-S battery with primitive Li anode shows a capacity of 452.2 $mAh.g^{-1}$ at 0.2C with a capacity retention of only 37.2%. It is noticeable that the average coulombic efficiency of Li-S battery with protected Li anode is as high as 91.4% in the electrolyte without $LiNO_3$, which is much higher than that of 80.7% for Li-S battery with primitive Li anode. Moreover, the Li-S battery with the protected Li anode also shows excellent prolonged cycle performance at 0.5C. Over 500 cycles, the capacity retention of 71.1% (from 1087.2 to 773 $mAh.g^{-1}$) is obtained, the decay rate is as low as 0.0578% per cycle, and the average coulombic efficiency is 92.3%. The charge/discharge profiles of the battery with protected Li anode are displayed in Fig.S4. There is no evident evolution of the curves during the prolonged cycles, indicating the highly reversibility of electrochemical reaction during the charge/discharge process. Although the addition of $LiNO_3$ in the electrolyte can increases the coulombic efficiency of Li-S battery, it was reported that $LiNO_3$ was reduced on the cathode below 1.5 V, and that the formed products severely affected the reversibility of sulfur cathode. Moreover, it is gradually consumed on the Li anode, which leads to a decrease in the protection efficiency, and it is a strong oxidative agent, which could cause a safety issue when a high concentration is used, especially at high temperature[10]. The Li-S battery with $Li_3N$ modified Li anode shows excellent cycle stability and improved coulombic efficiency in the electrolyte without $LiNO_3$. which can avoid the disadvantages of $LiNO_3$ additives.

Because lithium polysulfides are dissolved in the ethers-based electrolyte once formed, and they will migrate in the electrolyte and reach the surface of lithium anode, followed by immediate reaction with metallic-lithium anode and the formation of $Li_2S/Li_2S_2$[21]. It results in the rapid loss of the active material and serious anode corrosion. Therefore, the self-discharge of Li-S battery is much more serious than those of the conventional Li-ion batteries. However, as seen in Fig.S5, the self-discharge behavior is effectively suppressed by the protection of Li anode with $Li_3N$.

As shown in Fig.S6, $Li_3N$ layer on the surface of lithium anode restricts the contact of lithium anode and lithium polysulfides, the suppressed corrosive reaction promotes more lithium polysulfides to be reutilized at the following cycles, thus the redistribution of insulating active material are suppressed effectively. Therefore, the decreased resistance is obtained for the Li-S battery with $Li_3N$ protected Li anode after 100 cycles.

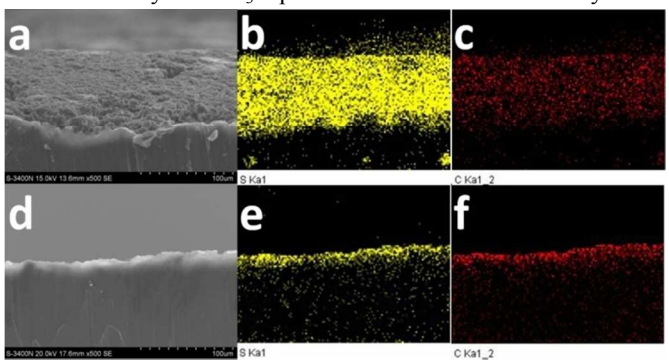


**Figure. 4** The cross section morphologies (a, d) and EDS mapping element of sulfur (b, e) and carbon (c, f) of primitive Li anode and $Li_3N$ protected Li anode after 100 cycles.

Fig. S7 compares the surface morphologies of the Li anode with and without $Li_3N$ protection layer after 100 cycles. The corrosive reaction between lithium polysulfides and Li anode results is severe during charge/discharge process for primitive Li anode, which increases the resistance of the battery and accelerates the capacity fading. As seen in Fig.4a, Fig.4b and Fig.4c, the thickness of $Li_2S_2/Li_2S$ layer on the surface of primitive lithium anode is as high as 100 μm，and the interface between Li and $Li_2S_2/Li_2S$ layer is uneven[24]. However, as seen in Fig.4d, Fig.4e and Fig.4f, the thickness of $Li_2S_2/Li_2S$ layer is only about 10 μm in the protected Li anode, only about 1/10 that of primitive lithium anode. In addition, the contact area between the $Li_3N$ protected Li anode and the $Li_2S/Li_2S_2$ layer are relatively trim, indicating that the undesired corrosive reaction is suppressed effectively when the lithium anode is protected by $Li_3N$ layer.

**Conclusions**

In summary, $Li_3N$ protection layer is successfully fabricated on the surface of Li anode through a simple and novel method at room temperature. The protected Li anode show high stability in the electrolyte compared with the primitive Li anode. As the anode of Li-S battery, the protected Li shows an enhanced cycle performance. Firstly, the protective layer has high $Li^+$ conductivity, which does not affect the diffusion kinetics of $Li^+$. Secondly, the $Li_3N$ layer on the surface of Li anode is beneficial to suppress the undesired side reactions between the Li anode and the electrolyte, forming a smooth and less resistive SEI. Thirdly, the $Li_3N$ layer can separate the contact between Li metal and lithium polysulfides, thus the corrosive reaction between them is inhibited effectively. Finally, the protective layer on the surface of Li anode can suppress the growth of Li dendrites originating from an no uniform deposition of Li, improving the safety of Li-S battery.

This work was financially supported by NSFC Project No. 51373195, No. 51201177 and No. 51272267; research projects from the Science and Technology Commission of Shanghai Municipality No. 08DZ2210900.

## Notes and references

[a] CAS Key Laboratory of Materials for Energy Conversion,
Shanghai Institute of Ceramics, Chinese Academy of Sciences,
Shanghai, China, 200050
Tel: +86-21-52411704;Fax: +86-21-52413903;
E-mail: zywen@mail.sic.ac.cn

† Electronic Supplementary Information (ESI) available: [details of any supplementary information available should be included here]. See DOI: 10.1039/b000000x/

1. S. A. F. Peter G. Bruce, Laurence J. Hardwick and Jean-Marie Tarascon, Nat Mater. 2012, 11(1), 19.
2. H B. Dunn, H. Kamath, J. M. Tarascon, Science. 2011, 334(6058), 928.
3. X. Ji and L. F. Nazar, J Mater Chem, 2010, 20, 9821.
4. J. W. Kim, J. D. Ocon, D. W. Park, J. Lee. ChemSusChem. 2014, 7(5), 1265
5. H. Kim, H.-D. Lim, J. Kim and K. Kang, Journal of Materials Chemistry A, 2014, 2, 33.
6. Y. Yang, G. Zheng and Y. Cui, Chem Soc Rev, 2013, 42, 3018.
7. Y. X. Yin, S. Xin, Y. G. Guo, L. J. Wan, Angewandte Chemie International Edition. 2013, 52(50), 13186.
8. Y. Fu. A. Manthiram, Y. S. Su, Accounts Chem Res. 2012, 46(5), 1125.
9. S. E. A. L. F. NAZAR, Accounts Chem Res. 2012, 46(5), 1135.
10. S. S. Zhang, Journal of Power Sources 2013, 231, 153.
11. Y. Diao, K. Xie, X. Hong and S. Xiong, Acta Chim Sinica, 2013, 71, 508.
12. X. Chen, Z. Xiao, X. Ning, Z. Liu, Z. Yang, C. Zou, S. Wang, X. Chen, Y. Chen, S. Huang, Adv Energy Mater. 2014, DOI: 10.1002/aenm.201301988;
13. G.-C. Li, G.-R. Li, S.-H. Ye and X.-P. Gao, Adv Energy Mater, 2012, 2, 1238.
14. X. L. Ji, K. T. Lee and L. F. Nazar, Nat Mater, 2009, 8, 500.
15. J. Zhang, H. Ye, Y. Yin and Y. Guo, Journal of Energy Chemistry, 2014, 23, 308.
16. X. Liang, Z. Y. Wen. Y. Liu, M. F. Wu, J. Jin, H. Zhang, X. W. Wu, J Power Sources. 2011, 196, 9839.
17. I. S. Kang, Y. S. Lee and D. W. Kim, Journal of the Electrochemical Society, 2013, 161, A53.
18. D. J. Lee, H. Lee, J. Song, M. H. Ryou, Y. M. Lee, H. T. Kim, J. K. Park, Electrochem Commun, 2014, 40, 45
19. J. B. Goodenough and K.-S. Park, J Am Chem Soc, 2013, 135, 1167-1176.
20. R. D. Rauh, K. M. Abraham, G. F. Pearson, J. K. Surprenant and S. B. Brummer, Journal of the Electrochemical Society, 1979, 126, 523.
21. Y. V. Mikhaylik and J. R. Akridge, Journal of the Electrochemical Society, 2004, 151, A1969.
22. D. Aurbach, E. Pollak, R. Elazari, G. Salitra, C. S. Kelley and J. Affinito, Journal of the Electrochemical Society, 2009, 156, A694.
23. S. S. Zhang, J Power Sources, 2013, 231, 153.
24. J. Zheng, M. Gu, M. J. Wagner, K. A. Hays, X. Li, P. Zuo, C. Wang, J. G. Zhang, J. Liu and J. Xiao, Journal of the Electrochemical Society, 2013, 160, A1624.
25. R. Demir-Cakan, M. Morcrette, Gangulibabu, A. Guéguen, R. Dedryvère and J.-M. Tarascon, Energ Environ Sci, 2013, 6, 176.
26. Y. M. Lee, N.-S. Choi, J. H. Park and J.-K. Park, J Power Sources, 2003, 119-121, 964.
27. B. Duan, W. Wang, H. Zhao, A. Wang, M. Wang, K. Yuan, Z. Yu and Y. Yang, ECS Electrochemistry Letters, 2013, 2, A47.
28. U. v. Alpen, A. Rabenau and G. H. Talat, Appl Phys Lett, 1977, 30, 621.
29. M. Wu, Z. Wen, Y. Liu, X. Wang and L. Huang, J Power Sources, 2011, 196, 8091.
30. Y. Yan, J. Y. Zhang, T. Cui, Y. Li, Y. M. Ma, J. Gong, Z. G. Zong and G. T. Zou, The European Physical Journal B, 2008, 61, 397.
31. S. Cui, W. Feng, H. Hu, Z. Feng and Y. Wang, Solid State Commun, 2009, 149, 612.
32. Y.C. Chang, J.H. Jong, J. Chin. Inst. Chem. Eng. 2004, 35 425.



 